Survey: Automatic Detection of Musculoskeletal Disorders from Radiographs

AMIRA GALAL

FARAH HISHAM

MENNATALLAH MOHAMED

SARA HASSAN

DR. AYMAN NABIL

ENG.TARAGGY GHANIM

18/12/2018

Introduction

- Musculoskeletal disorders (**MSDs**) are conditions that affect bones, joints and muscles.
- **MSDs** affect more than 1.7 billion people worldwide.

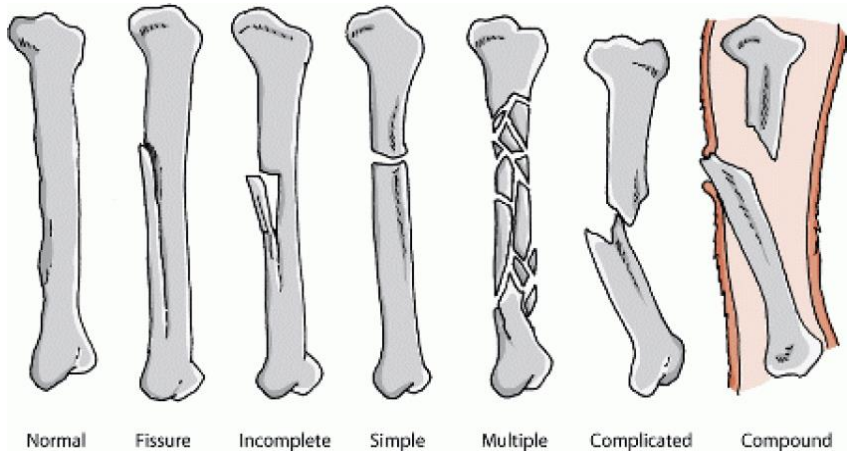

Fracture types

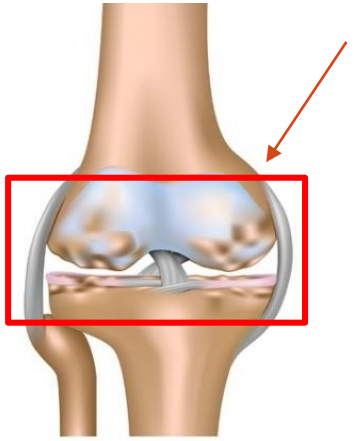

Osteoarthritis

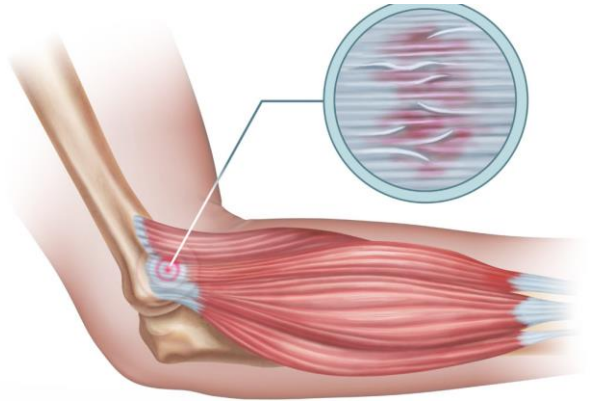

Tendinitis

Problem Statement

- Huge workload on radiologists can lead to misdiagnosis.
- Inexperience of staff.
- Unclear/poor quality radio-graphs.

*Bhargavan, Mythreyi and Sunshine, Jonathan H. Utilization of radiology services in the united states: levels and trends in modalities, regions, and populations. Radiology, 234(3):824–832, 2005.

Preview

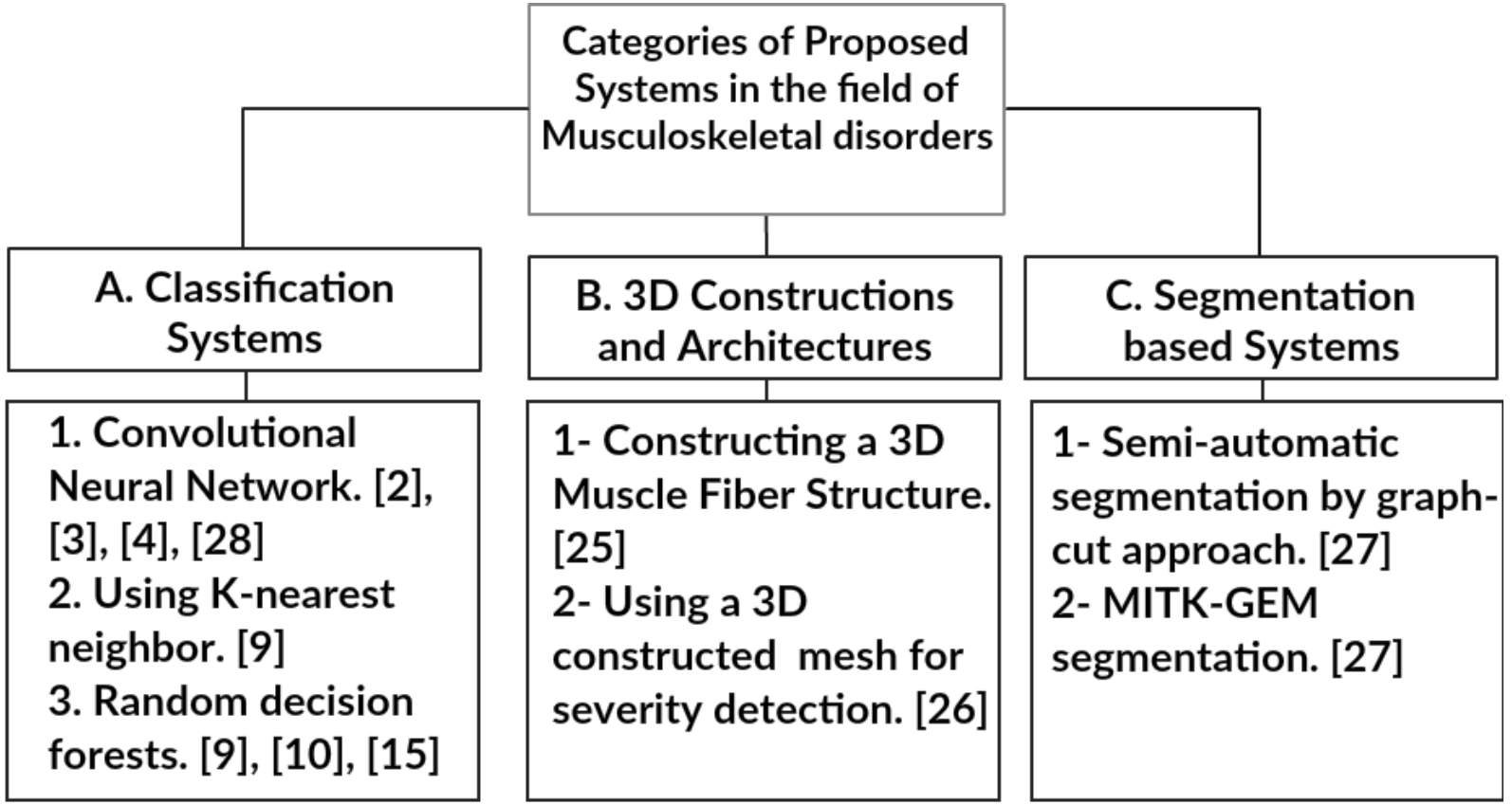
Categories of Proposed Systems in the field of Musculoskeletal disorders
A. Classification Systems
B. 3D Constructions and Architectures
C. Segmentation based Systems
1. Convolutional Neural Network. [2], [3], [4], [28]
2. Using K-nearest neighbor. [9]
3. Random decision forests. [9], [10], [15]
1- Constructing a 3D Muscle Fiber Structure. [25]
2- Using a 3D constructed mesh for severity detection. [26]
1- Semi-automatic segmentation by graph-cut approach. [27]
2- MITK-GEM segmentation. [27]

MURA (1 / 2): Large Dataset for Abnormality Detection in Musculoskeletal Radiographs

- Large dataset containing 40,561 images of the upper-limb extremity
- 169-layered CNN model(Dense Convolutional Network architecture)
- Classifies image as either normal or abnormal

Normal

Abnormal

MURA (2/2)

	Radiologist 1	Radiologist 2	Radiologist 3	Model
Elbow	0.850 (0.830, 0.871)	0.710 (0.674, 0.745)	0.719 (0.685, 0.752)	0.710 (0.674, 0.745)
Finger	0.304 (0.249, 0.358)	0.403 (0.339, 0.467)	0.410 (0.358, 0.463)	0.389 (0.332, 0.446)
Forearm	0.796 (0.772, 0.821)	0.802 (0.779, 0.825)	0.798 (0.774, 0.822)	0.737 (0.707, 0.766)
Hand	0.661 (0.623, 0.698)	0.927 (0.917, 0.937)	0.789 (0.762, 0.815)	0.851 (0.830, 0.871)
Humerus	0.867 (0.850, 0.883)	0.733 (0.703, 0.764)	0.933 (0.925, 0.942)	0.600 (0.558, 0.642)
Shoulder	0.864 (0.847, 0.881)	0.791 (0.765, 0.816)	0.864 (0.847, 0.881)	0.729 (0.697, 0.760)
Wrist	0.791 (0.766, 0.817)	0.931 (0.922, 0.940)	0.931 (0.922, 0.940)	0.931 (0.922, 0.940)
Overall	0.731 (0.726, 0.735)	0.763 (0.759, 0.767)	0.778 (0.774, 0.782)	0.705 (0.700, 0.710)

- Compared model's performance to radiologists' performance
- Best score achieved on wrist and finger

CNN

	Automatic Knee Osteoarthritis Diagnosis from Plain Radiographs: A Deep Learning based Approach	Segmentation of Pathological Spines in CT Images Using a Two-Way CNN and a Collision-Based Model	ShapeAware Deep Convolutional Neural Network for Vertebrae Segmentation
Method	Siamese architecture on convolutional neural network (CNN). Measured by Kellgren Lawrence (KL)	Classification of 3 segmentation classes using CNN. Initialization of a collision based model which was a mesh union of 2 successive vertebra.	The UNet architecture for extracting different objects.
Dataset	Multicenter osteoarthritis study (MOST) dataset.	Images of normal spines collected from clinics.	Images of 792 vertebrae patches collected from clinics.
Results	Quadratic kappa coefficient of 0.83 and average multiclass accuracy of 66.71%. AUC (area under the curve) of 0.93 in a ROC (Receiver operator curve) curve.	Dice similarity coefficient (DSC) 93.2 ± 2.2%mm, mean symmetric surface distance (MSD) 0.5 ± 0.2mm, and Hausdorff surface distance (HD) 8.4 ± 3.4mm.	Reduced the average error by 12% achieving the best error of 0.99 pixels. A maximum average pixel-level segmentation accuracy of 97.01%.

Random Forest

	Classification of Osteoporotic Vertebral Fractures Using Shape and Appearance Modelling	Unfolded Cylindrical Projection for Rib Fracture Diagnosis	Automatic Localization of the Lumbar Vertebral Landmarks in CT Images with Context Features
Method	Appearance modelling combined with K-nearest neighbors and random forest classifiers	Detection of anatomical landmarks using Random Forest (RF) classifier trained by histogram of oriented gradients (HOG)	Two levels of Random Forest regression technique were applied. First layer was applied on appearance features and the second layer was on context feature.
Dataset	369 CT were used for landmark classifier training, and another dataset for testing	369 CT datasets for landmark classifier training and 70 testing.	28 lumbar-focused computed tomography images
Results	Accuracy improved as the false positive decreased by 60% having sensitivity of 80%	The qualitative evaluation resulted in 0.0% gold standard, 62.9% diagnostic confidence, 21.4% moderate confidence, 10.0% low-level of confidence, and 5.7% very low-level of confidence	Detection of landmarks with a mean localization error of 3.0 mm

3D Architecture

	Reconstruction of 3D Muscle Fiber Structure Using High Resolution Cryosectioned Volume	3D Cobb Angle Measurements from Scoliotic Mesh Models with Varying Face-Vertex Density
Method	Correction of artifact which was a discontinuity of the color balance.	Detecting the severity level of the deformity in spine was done by measuring the 3D cobb angle.
Dataset	Visible Korean Human dataset	60 mesh models with spinal deformity.
Results	Successful identification of each muscle fiber in the two given datasets (female and male).	Accuracy on faces having mean edge less than 6mm of 3.0° absolute mean error which is equivalent to 2.2° standard deviation.

Public Datasets

Dataset	Study Type	Images
MURA	Musculoskeletal (Upper Extremity)	40,561 (Elbow:1912)
Osteo Arthritis Initiative (OAI)	Musculoskeletal (Knee)	8,892
Multicenter Osteoarthritis Study (MOST)	Musculoskeletal (Knee)	18,376
Visible Korean Human	Human Anatomy (Cadaver)	5000+
ChestX-ray14	Chest	112,120

Conclusion

- CNN is commonly used, giving promising results.
- CNN is used in different ways, such as image segmentation and detecting abnormalities.
- The available labeled datasets are not enough.
- Reached accuracy levels leave room for enhancement.

amira1504361@miuegypt.edu.eg
farah1502451@miuegypt.edu.eg
mennatallah1500885@miuegypt.edu.eg
sara1502749@miuegypt.edu.eg
taraggy.ghanim@miuegypt.edu.eg
ayman.nabil@miuegypt.edu.eg

References

*R. Korez, B. Likar, F. Pernuš, T. Vrtovec, Segmentation of pathological spines in ct images using a two-way cnn and a collision-based model, in: International Workshop and Challenge on Computational Methodsand Clinical Applications in Musculoskeletal Imaging, Springer, 2017, pp. 95–107.

*S. M. R. Al Arif, K. Knapp, G. Slabaugh, Shape-aware deep convolutional neural network for vertebrae segmentation, in: International Workshop and Challenge on Computational Methods and Clinical Applications in Musculoskeletal Imaging, Springer, 2017, pp. 12–24.

*A. Rasoulian, R. Rohling, P. Abolmaesumi, Lumbar spine segmentation using a statistical multi-vertebrae anatomical shape+ pose model, IEEE transactions on medical imaging 32 (10) (2013) 1890–1900.

*P. A. Bromiley, E. P. Kariki, J. E. Adams, T. F. Cootes, Classification of osteoporotic vertebral fractures using shape and appearance modelling, in: International Workshop and Challenge on Computational Methods and Clinical Applications in Musculoskeletal Imaging, Springer, 2017, pp. 133–147.

*D. Damopoulos, B. Glocker, G. Zheng, Automatic localization of the lumbar vertebral landmarks in ct images with context features, in: International Workshop and Challenge on Computational Methods and Clinical Applications in Musculoskeletal Imaging, Springer, 2017, pp. 59–71.

*http://www.boneandjointburden.org/fourth-edition/i1/big-picture

References

*C. Tobon-Gomez, T. Stroud, J. Cameron, D. Elcock, A. Murray, D. Wyeth, C. Conway, S. Reynolds, P. A. G. Teixeira, A. Blum, et al., Unfolded cylindrical projection for rib fracture diagnosis, in: International Workshop and Challenge on Computational Methods and Clinical Applications in Musculoskeletal Imaging, Springer, 2017, pp. 36–47.

*A. Tiulpin, J. Thevenot, E. Rahtu, P. Lehenkari, S. Saarakkala, Automatic knee osteoarthritis diagnosis from plain radiographs: a deep learning-based approach, Scientific reports 8 (1) (2018) 1727.

*K. R. P. S. K. S. . V. T. PetkoviÄGˇ , U., 3d cobb angle measurements from scoliotic mesh models with varying face-vertex density, in: International Workshop and Challenge on Computational Methods and Clinical Applications in Musculoskeletal Imaging, Springer, 2017, pp. 48–58.

*Y. Otake, K. Miyamoto, A. Ollivier, F. Yokota, N. Fukuda, L. J. Oâˇ A ´ ZDonnell, C.-F. Westin, M. Takao, N. Sugano, B. S. Chung, et al., Reconstruction of 3d muscle fiber structure using high resolution cryosectioned volume, in: International Workshop and Challenge on Computational Methods and Clinical Applications in Musculoskeletal Imaging, Springer, 2017, pp. 85–94.

*P. Rajpurkar, J. Irvin, A. Bagul, D. Ding, T. Duan, H. Mehta, B. Yang, K. Zhu, D. Laird, R. L. Ball, et al., Mura dataset: Towards radiologistlevel abnormality detection in musculoskeletal radiographs.

*C. Tobon-Gomez, T. Stroud, J. Cameron, D. Elcock, A. Murray, D. Wyeth, C. Conway, S. Reynolds, P. A. G. Teixeira, A. Blum, et al., Unfolded cylindrical projection for rib fracture diagnosis, in: International Workshop and Challenge on Computational Methods and Clinical Applications in Musculoskeletal Imaging, Springer, 2017, pp. 36–47.